ChemComm

COMMUNICATION

View Article Online
View Journal | View Issue

Cite this: *Chem. Commun.*, 2023, **59**, 1975

Received 26th November 2022,
Accepted 22nd January 2023

DOI: 10.1039/d2cc06415d

rsc.li/chemcomm

Intimate relationship between C–I reductive elimination, aryl scrambling and isomerization processes in Au(III) complexes†

Sara Fernández-Moyano, Guillermo Marcos-Ayuso, Marconi N. Peñas-Defrutos, * Camino Bartolomé and Pablo Espinet *

^{19}F NMR monitoring shows that heating *trans*-$[Au^{III}Rf_2I_2]^-$ solutions (Rf = $C_6F_3Cl_2$-3,5) leads to formation of *cis*-$[AuRf_2I_2]^-$, $[AuRf_3I]^-$ and $[AuRfI_3]^-$ *via* kinetic competition between isomerization and Rf/I scrambling. The system evolution is driven by the easy Rf–I reductive elimination from $[AuRfI_3]^-$ (forming also $[AuI_2]^-$), which is faster than any of the Rf–Rf couplings from the coexisting species, hindering the commonly desired and thermodynamically preferred C–C coupling. A kinetic model where I^- dissociation triggers both isomerization and transmetalation steps is proposed, which fits well the experimental data. DFT calculations support that the lower bond strength of Au^{III}–I compared to other halides produces a pathway switch that makes C–I coupling kinetically preferred. Consequently, it is better avoided in reactions looking for C–C coupling.

In the recent years, C–C cross coupling based on the Au^{III}/Au^{I} pair has become a hot topic as a potential alternative to Pd^{II}/Pd^{0} chemistry.[1,2] Efficient aryl–aryl coupling processes mediated by gold systems,[3] including one example of the more challenging Ar^F–Ar^F (Ar^F = perhaloaryl group) reductive elimination (RE) from well-defined Au(III) complexes have been reported.[4,5] In this context we planned to prepare *cis*-$Au^{III}Rf_2$ adducts (Rf = $C_6F_3Cl_2$-3,5) to study the C–C coupling possibilities, as we did previously with *cis*-$[Pd^{II}Pf_2L^n]$ (Pf = C_6F_5) species.[6] For this mechanistic study we use Rf aryl complexes, which display simple and clean ^{19}F NMR spectra.

We recently reported that, trying to synthesize $(\mu\text{-Cl})_2[AuRf_2]_2$, an unexpected Rf/Cl scrambling process was observed (Scheme 1, above).[7] There are just a few reported cases of aryl scrambling phenomena involving Au(III) complexes. Those reported by Luzuriaga[8] (Scheme 1, middle) and Nevado[9] groups (Scheme 1, below), have in common that they are only detected when strong oxidants come into play, and are lacking any mechanistic investigation.

In the case of our previous study (Scheme 1, above), the scrambling occurs in more conventional conditions, and is triggered by halide abstraction from *trans*-$[AuRf_2Cl_2]^-$ (**1-Cl**) with 1 equiv. of $AgClO_4$. Evaporation of the solvent (specifically Et_2O) and dissolution in the non-coordinating $CHCl_3$ reverted the scrambling forming the intended dimer $(\mu\text{-Cl})_2[AuRf_2]_2$.[7] The reaction conditions precluded to obtain kinetic information, but the drastically different outcome observed when using *cis*-$[AuRf_2Cl_2]^-$ (**2-Cl**) (no scrambling detected) supported satisfactorily our mechanistic proposal of kinetic competition between isomerization and scrambling from the unstable *trans*-$[AuRf_2Cl(solv)]$.[7] Moreover, it is worth noting that, upon heating, solutions of **1-Cl** led selectively to the *cis* complex **2-Cl**, which is reluctant to undergo coupling. On the contrary, accessible Rf–Rf reductive elimination (RE) barriers were observed for *cis*-$[AuRf_2Cl(L)]$ (L = μ-Cl, OEt_2) derivatives, while no traces of Rf–Cl (hypothetically resulting from a C–Cl coupling) were detected in any case.[7]

In this context, here we study the surprising reactivity displayed by solutions of the iodo-complex (NBu_4)*trans*-$[AuRf_2I_2]$ (**1**) in poorly coordinating solvents. Complex **1** was obtained in excellent yield by oxidation of $(NBu_4)[AuRf_2]$,[10] with I_2 (see details in ESI†).

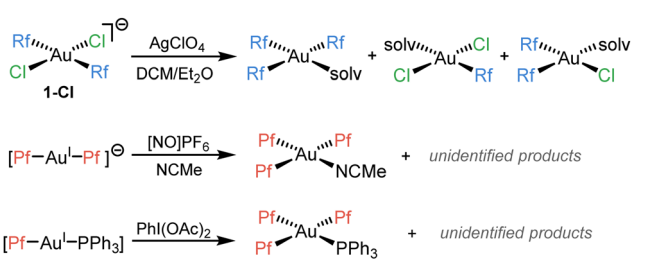

Scheme 1 Reported cases of aryl scrambling involving Au^{III} complexes.

IU CINQUIMA/Química Inorgánica, Facultad de Ciencias, Universidad de Valladolid, Valladolid 47071, Spain. E-mail: marconi_44@hotmail.com, espinet@qi.uva.es

† Electronic supplementary information (ESI) available: Synthesis and characterization of the complexes including NMR spectra, microkinetic model, computational details and X-ray data. CCDC 2221886–2221889. For ESI and crystallographic data in CIF or other electronic format see DOI: https://doi.org/10.1039/d2cc06415d

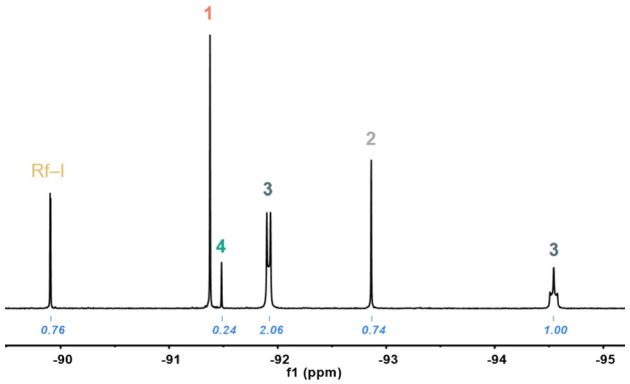

Fig. 1 F_{ortho} region of the ^{19}F NMR spectrum recorded from solutions of **1** in TCE-d_2 after heating at 323 K for 1 day. Assignment of the signals and corresponding integrals.

The synthesis of *cis*-$[AuPf_2I_2]^-$ (Pf = C_6F_5), by heating the *trans* complex in CH_2Cl_2, was reported long ago (without ^{19}F NMR data), but we confirmed that a clean isomerization does not occur in those conditions (see Fig. S1, ESI†).[11] Similarly, the behaviour of **1** in tetrachloroethane (TCE) solution is not simple.[12] Instead of leading selectively to (NBu_4)*cis*-$[AuRf_2I_2]$ (**2**), as it might be expected by analogy with the Cl complexes, a mixture of several species bearing Rf groups was observed by ^{19}F NMR (Fig. 1 and Fig. S3, ESI†).

The two chemically inequivalent F_{ortho} signals in 2 : 1 ratio and displaying multiplicity are consistent with $(NBu_4)[AuRf_3I]$ (**3**), a square-planar species formed presumably by Rf/I scrambling. The pseudo doublet and triplet multiplicities of the F_{ortho} signals reveal hindered rotation of the three Rf groups,[13] imposed by the bulky iodo group, since when fast rotation is allowed, as reported for $[AuRf_3(OH_2)]$,[7] triplet and quintet signals with relative integrals 2 : 1 are found. Complex **3** could be selectively synthesized by reaction of $[AuRf_3(OH_2)]$ with $(NBu_4)I$ and was fully characterized (details in ESI,† see Fig. S7 for its X-ray structure).

The F_{ortho} resonance at −89.9 ppm (doublet, 2F) and the F_{para} signal at −108.1 ppm (triplet, 1F), correspond to the organic Rf–I, which must be the result of C–I reductive elimination, while no traces of Rf–Rf were observed. Interestingly, this C–I coupling seems to be fast at 323 K in contrast with the remarkably slow C–C RE observed for **2-Cl** at 393 K in TCE. For stoichiometry reasons, the concentrations of tris-aryl and mono-aryl species must be identical, and consequently we assign the signal at −91.5 ppm to $(NBu_4)[AuRfI_3]$ (**4**). Finally, the signal at −92.9 ppm corresponds to (NBu_4)*cis*-$[AuRf_2I_2]$ (**2**). The identity of the latter was confirmed by reaction of **2-Cl** with excess of KI (details in ESI,† see also Fig. S4).

After prolonged heating of **1** for 2 days at 353 K in TCE, the final products of the reaction were **3** + Rf–I, in 1 : 1 ratio, by ^{19}F NMR. Obviously, some gold (specifically half of it) was missing, but we were able to crystallize from the reaction mixture the Au^I complex $(NBu_4)[AuI_2]$ (**5**) blind to ^{19}F NMR. This adjusts the chemical balance (Scheme 2). It is worth noting that signals of both bis-aryl complexes **1** and **2** disappear, confirming the scrambling completeness (Fig. S5, ESI†).

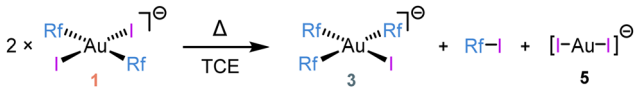

Scheme 2 Final outcome of the reaction of **1** in TCE. Products are formed after heating 2 days at 353 K.

For better understanding of this remarkable reactivity, the evolution of **1** in TCE-d_2 at 338 K was monitored by ^{19}F NMR. The concentration *vs.* time data plot obtained for the different species is shown in Fig. 2 (dots are the experimental data). The kinetics of the competitive processes occurring is not trivial. Clearly, an induction period is observed in the disappearance of **1**, meaning that either an intermediate or a product is catalysing the transformation. The addition of complexes **3**, **5** or the organic molecule Rf–I did not affect the rate of the reaction and the curve of complex $(NBu_4)[AuRfI_3]$ (**4**) confirms that it is thermodynamically unstable and behaves as the intermediate that gives rise to Rf–I + $(NBu_4)[AuI_2]$ (**5**) by C–I reductive elimination (Scheme 2).

The isomerization in gold(III) systems has been proposed to follow a dissociative + topomerization mechanism.[14] Transmetalation reactions (scrambling is one of them) typically require ligand dissociation in square-planar complexes.[15] Interestingly, addition of substoichiometric amounts of $(NBu_4)I$ to solutions of **1**, specifically 20 mol% in identical conditions to the experiment in Fig. 2 (TCE-d_2, 338 K, 15 h), suppresses the reactivity. This supports a dissociative mechanism, where I^- coordination sequesters low concentration intermediates.[16]

The reaction evolution was satisfactorily fitted using COPASI software (see microkinetic details in ESI†) and the simplified kinetic model depicted in Scheme 3, which involves dissociative steps. Only six elemental reactions were needed to reproduce the experimental data precisely (see continuous lines in Fig. 2).

The pair of reactions ***A*/*B*** in Scheme 3 accounts for the induction period observed in the disappearance of **1** (orange trace, Fig. 2). We propose that iodide dissociation from the reactant, forming an unobservable tricoordinate intermediate

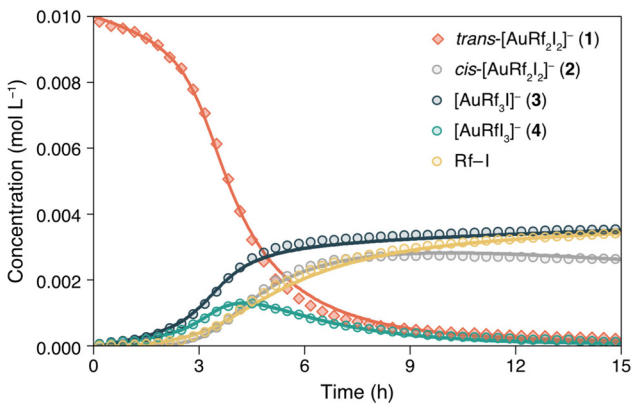

Fig. 2 Concentration *vs.* time plot of experimental data (dots) obtained by ^{19}FNMR monitoring and COPASI-fitted values (continuous lines) of the fluorinated-species observed when heating complex **1** in TCE-d_2 at 338 K.

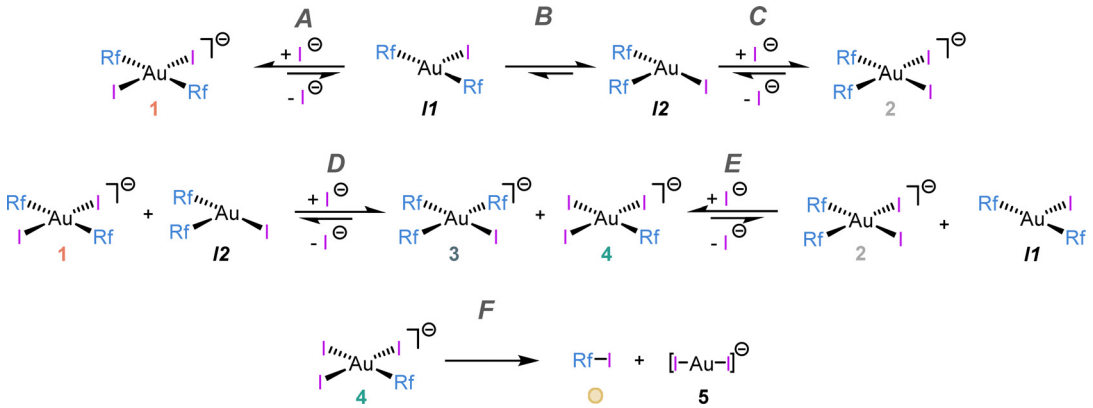

Scheme 3 Kinetic model used for the non-linear fitting shown in Fig. 2. Elemental reactions are labelled with letters (***A–F***).

I1, triggers the process.[17] Obviously, the first equilibrium ***A*** is very disfavoured thermodynamically. On the contrary, isomerization from the *trans*-intermediate ***I1*** leading to a more stable *cis* tricoordinate species labelled as ***I2*** must be exergonic, attending to *trans* influence reasons (step ***B***). The latter, ***I2***, reacts with the initial complex **1** catalysing its consumption forming the scrambling species **3** and **4** by Rf/I transmetalation (Scheme 3***D***, dark and light green lines in Fig. 2).[18] It is worth remarking that the preferred reactivity combining *trans* with *cis* 3- and 4-coordinated species was also proposed in our previous report.[7]

Scheme 3***C*** shows the capture of ***I2*** by iodide coordination forming the *cis* anionic complex **2**, which kinetically competes with the scrambling shown in reaction ***D***. At long reaction times, complex **2** slowly disappears (grey line in Fig. 2) by reaction with the minute amount of ***I1*** present in solution (reaction ***E***). This plausible scrambling process leads as well to **3** + **4**, similarly to the **1** + ***I2*** reaction.

The last reaction of the kinetic model (step ***F***) is the irreversible C–I coupling from **4**, producing Rf–I (yellow line in Fig. 2) + **5**. This reductive elimination step is the driving force bringing the reaction, at longer times or higher temperature, to the final products shown in Scheme 2, which is satisfactorily reproduced by our kinetic model (see Fig. S12, ESI†). The key role of iodide dissociation in the model is fully supported by the lethal effect of addition of substoichiometric $(NBu_4)I$ on the reactivity.

Although there are several other potential sources of Rf–I coupling in the mixture (**1**, **2**, **3**), the good COPASI fitting of the model supports that the only Rf–I reductive elimination energetically accessible in the experimental conditions (338 K) occurs on $[AuRfI_3]^-$ (**4**). On the other hand, complexes **2** and **3** have Rf groups in *cis* arrangement that could undergo Rf–Rf coupling, but this biphenyl was not observed in any case.

For further support of the kinetic conclusions, we performed DFT calculations (see ESI† for details). The thermodynamic (ΔG) and kinetic ($\Delta G^{\ddagger}$) computational results of the possible C–I and C–C RE processes from complexes **1–4** and selected data from the Cl analogues **2-Cl** and **4-Cl** for comparison, are given in Table 1.

Table 1 Thermodynamic data (ΔG) of the possible C–X (X = I, Cl) and C–C couplings from $[AuRf_nX_{4-n}]^-$ complexes with their activation energies ($\Delta G^{\ddagger}$) in kcal mol^{-1}

Entry	Comp.	RE type	Products	ΔG	$\Delta G^{\ddagger}$
1	**1**	C–I	Rf–I + $[AuRfI]^-$	−3.0	+37.3
2	**2**	C–I	Rf–I + $[AuRfI]^-$	−1.6	+35.4
3	**3**	C–I	Rf–I + $[AuRf_2]^-$	+6.4	+48.3
4	**4**	C–I	Rf–I + $[AuI_2]^-$	−9.6	**+22.8**
5	**2**	C–C	Rf–Rf + $[AuI_2]^-$	−35.0	+26.6
6	**3**	C–C	Rf–Rf + $[AuRfI]^-$	−29.9	+35.0
7	**4-Cl**	C–Cl	Rf–Cl + $[AuCl_2]^-$	−12.0	+31.5
8	**2-Cl**	C–C	Rf–Rf + $[AuCl_2]^-$	−31.1	+29.0

Entries 1–4 contain the computed data for the possible C–I RE processes from the mixture of species in Fig. 1, revealing that the coupling from complex **3** is thermodynamically disfavoured (ΔG = +6.4 kcal mol^{-1}).[19] Besides, Rf–I extrusion is only scarcely exergonic from **1** and **2** (entries 1 and 2). Remarkably, the concerted C–I RE from the electron poorest species,[20] namely $[AuRfI_3]^-$ (**4**), is both the most thermodynamically favoured Rf–I coupling (*i.e* −9.6 kcal mol^{-1}, it may indeed be considered irreversible) and, more importantly, the fastest process in Table 1 ($\Delta G^{\ddagger}$ = +22.8 kcal mol^{-1}, entry 4). The stabilizing effect of $[AuI_2]^-$ (**5**) + Rf–I formation drives the equilibria in Scheme 3 to scrambling completeness. The remaining non-used groups make up $[AuRf_3I]^-$ (**3**), and the outcome shown in Scheme 2.

The Rf–Rf coupling, which is by far the most thermodynamically favoured (entries 5 and 6) is absent of the reaction for kinetic reasons: the $\Delta G^{\ddagger}$ values computed for the Rf–Rf coupling processes from **2** and **3** (the only species with Rf groups arranged *cis*) are clearly higher than C–I from **4** (*i.e* +26.6 kcal mol^{-1} in entry 5), or inaccessible (entry 6).[21] Fig. S8 (ESI†) shows the associated transition states optimized for both competing processes.

Replacing I by Cl (entries 7 and 8), the significant kinetic preference for Rf–I *vs.* Rf–Rf coupling is reverted. While both ΔG and $\Delta G^{\ddagger}$ values for Rf–Rf formation from *cis*-$[AuRf_2Cl_2]^-$ (**2-Cl**) are similar to those found from the I-analogue **2**, the activation barrier for the C–Cl coupling from a hypothetical

$[AuRfCl_3]^-$ (**4-Cl**) is clearly higher ($\Delta G^{\ddagger}$ = +29.0 *vs.* +31.5 kcal mol^{-1}) highlighting the key role of the halide. Besides, the deep stability of complex **2-Cl** makes the eventual scrambling thermodynamically highly disfavoured. The Au^{III}–X elongation required to reach the C–X coupling TS is more demanding for the stronger Au^{III}–Cl bond (8.7 kcal mol^{-1} $\Delta G^{\ddagger}$ difference between entries 4 and 7).[19a,22]

We also confirmed experimentally that the behaviour of **1-Br** is analogue to **1-Cl**, and isomerizes to **2-Br** (that eventually undergoes Rf–Rf coupling under harsh conditions), while no traces of Rf/Br scrambling are detected (see ESI† for details).

Finally, the narrow energy difference between *trans*-$[AuRf_2I_2]^-$ (**1**) and *cis*-$[AuRf_2I_2]^-$ (**2**) isomers (*i.e* −1.4 kcal mol^{-1}) contrasts with the selective isomerization observed for the Cl analogue (ΔG for **1-Cl**/**2-Cl** conversion is −10.5 kcal mol^{-1}). The latter is a reminder of the participation of opposite influences in simple isomeric structures: attending to the *transphobia* concept a *cis* arrangement should be preferred for both halides,[23] but the bulkiness of the iodo ligand plays an important destabilizing role on the *cis* isomer **2**,[24] making the Rf/I scrambling thermodynamically accessible in our case. This analysis warns that both crowding repulsive effects and electronic aspects need to be taken into account to rationalize some complex reactivity patterns.

In conclusion, the nature of the halide in $[AuRf_2X_2]^-$ complexes (X = Cl, Br, I) plays a decisive influence on the evolution of these species in solution. While the iodide compound undergoes Rf/I scrambling and feasible Rf–I coupling (pathway favoured by the comparative weakness of the Au^{III}–I bond), selective *trans*/*cis* isomerization and challenging Rf–Rf coupling is found for Cl and Br derivatives. This potentially problematic kinetic competition should be considered in the development of new Au catalysed C–C cross-coupling processes.

We thank the Spanish MCINN (Project PID2020-118547GB-I00) and the JCyL (Project VA224P20) for the funding provided. We acknowledge Miguel Claros and Eric Mates-Torres for help. M. N. P-D. thanks the UVa for a Margarita Salas fellowship (ref. CONVREC-2021-221).

Conflicts of interest

There are no conflicts to declare.

Notes and references

1 For reviews see: (*a*) V. W. Bhoyare, A. G. Tathe, A. Das, C. C. Chintawar and N. T. Patil, *Chem. Soc. Rev.*, 2021, **50**, 10422–10450; (*b*) A. Nijamudheen and A. Datta, *Chem. – Eur. J.*, 2020, **26**, 1442–1487; (*c*) C. Fricke, W. B. Reid and F. Schoenebeck, *Eur. J. Org. Chem.*, 2020, 7119–7130.
2 For general gold catalysed organic transformations see: (*a*) M. Joost, A. Amgoune and D. Bourissou, *Angew. Chem., Int. Ed.*, 2015, **54**, 15022–15045; (*b*) L. Rocchigiani and M. Bochmann, *Chem. Rev.*, 2021, **121**, 8364–8451.
3 (*a*) W. J. Wolf, M. S. Winston and F. D. Toste, *Nat. Chem.*, 2014, **6**, 159–164; (*b*) S. Kramer, *Synthesis*, 2020, 2017–2030.
4 K. Kang, S. Liu, T. Xu, D. Wang, X. Leng, R. Bai, Y. Lan and Q. Shen, *Organometallics*, 2017, **36**, 4727–4740.
5 For other cross-coupling reactions using stoichiometric perhaloroaryl gold complexes, see: (*a*) X. C. Cambeiro, T. C. Boorman, P. Lu and I. Larrosa, *Angew. Chem., Int. Ed.*, 2013, **52**, 1781–1784; (*b*) M. Hofer, E. Gomez-Bengoa and C. Nevado, *Organometallics*, 2014, **33**, 1328–1332.
6 E. Gioria, J. del Pozo, J. M. Martínez-Ilarduya and P. Espinet, *Angew. Chem., Int. Ed.*, 2016, **55**, 13276–13280.
7 S. Fernández-Moyano, M. N. Peñas-Defrutos, C. Bartolomé and P. Espinet, *Chem. Commun.*, 2021, **57**, 125–128.
8 A. T. Overton, J. M. López-de-Luzuriaga, M. E. Olmos and A. A. Mohamed, *Organometallics*, 2012, **31**, 3460–3462.
9 M. Hofer and C. Nevado, *Eur. J. Inorg. Chem.*, 2012, 1338–1341.
10 E. J. Fernández, A. Laguna, J. M. López-de-Luzuriaga, M. Monge, M. Montiel, M. E. Olmos, J. Pérez, R. C. Puelles and J. C. Sáenz, *Dalton Trans.*, 2005, 1162–1164.
11 R. Usón, A. Laguna, J. García and M. Laguna, *Inorg. Chim. Acta*, 1979, **37**, 201–207.
12 The behaviour in $CDCl_3$ is analogous (see Fig. S2, ESI†) but it does not allow to heat above 323 K as needed for kinetic monitoring. Aryl scrambling was also observed in other poorly coordinating solvents, such as toluene, but **1** is scarcely soluble in aromatic solvents.
13 P. Espinet, A. C. Albéniz, J. A. Casares and J. M. Martínez-Ilarduya, *Coord. Chem. Rev.*, 2008, **252**, 2180–2208.
14 (*a*) S. Komiya, T. A. Albright, R. Hoffmann and J. K. Kochi, *J. Am. Chem. Soc.*, 1976, **98**, 7255–7265; (*b*) A. Tamaki, S. A. Magennis and J. K. Kochi, *J. Am. Chem. Soc.*, 1974, **96**, 6140–6148.
15 (*a*) M. Gazvoda, M. Virant, B. Pinter and J. Kosmrlj, *Nat. Commun.*, 2018, **9**, 4814–4822; (*b*) M. H. Pérez-Temprano, J. A. Casares, A. R. de Lera, R. Álvarez and P. Espinet, *Angew. Chem., Int. Ed.*, 2012, **51**, 4917–4920.
16 C. Bartolomé, Z. Ramiro, M. N. Peñas-Defrutos and P. Espinet, *ACS Catal.*, 2016, **6**, 6537–6545.
17 Naked tricoordinate species are likely just fugacious. $[AuRf_2I(w)]$ intermediates (w = any adventitious labile ligand, such as the solvent), formed after I^- dissociation, are more plausible.
18 The kinetic model simplifies the Rf/I transmetalation as elemental reactions (***D***, ***E***). However, it probably proceeds *via* a multi-step mechanism featuring dimers with Rf and/or I bridges.
19 For oxidative addition of Ar–I to Au^I see: (*a*) J. A. Cadge, J. F. Bower and C. A. Russell, *Angew. Chem., Int. Ed.*, 2021, **60**, 24976–24983; (*b*) M. Joost, A. Zeineddine, L. Estévez, S. Mallet-Ladeira, K. Miqueu, A. Amgoune and D. Bourissou, *J. Am. Chem. Soc.*, 2014, **136**, 14654–14657; (*c*) Y. Yang, L. Eberle, F. F. Mulks, J. F. Wunsch, M. Zimmer, F. Rominger, M. Rudolph and A. S. K. Hashmi, *J. Am. Chem. Soc.*, 2019, **141**, 17414–17420; (*d*) I. Fernández, L. P. Wolters and F. M. Bickelhaupt, *J. Comput. Chem.*, 2014, **35**, 2140–2145.
20 K. Kang, S. Liu, C. Xu, Z. Lu, S. Liu, X. Leng, Y. Lan and Q. Shen, *Organometallics*, 2021, **40**, 2231–2239.
21 For C–C *vs.* C–X coupling competition see: (*a*) M. S. Winston, W. J. Wolf and F. D. Toste, *J. Am. Chem. Soc.*, 2015, **137**, 7921–7928; (*b*) R. Bhattacharjee, A. Nijamudheen and A. Datta, *Chem. – Eur. J.*, 2017, **23**, 4169–4179.
22 M. Baya, A. Pérez-Bitrián, S. Martínez-Salvador, A. Martín, J. M. Casa, B. Menjón and J. Orduna, *Chem. – Eur. J.*, 2018, **24**, 1514–1517.
23 J. Vicente, A. Arcas, D. Bautista and P. G. Jones, *Organometallics*, 1997, **16**, 2127–2138.
24 S. Coco, F. Díez-Expósito, P. Espinet, C. Fernández-Mayordomo, J. M. Martín-Álvarez and A. M. Levelut, *Chem. Mater.*, 1998, **10**, 3666–3671.

